REPORT 1020

MEASUREMENTS OF AVERAGE HEAT-TRANSFER AND FRICTION COEFFICIENTS FOR SUBSONIC FLOW OF AIR IN SMOOTH TUBES AT HIGH SURFACE AND FLUID TEMPERATURES [1]

By Leroy V. Humble, Warren H. Lowdermilk, and Leland C. Desmon

SUMMARY

An investigation of forced-convection heat transfer and associated pressure drops was conducted with air flowing through smooth tubes for an over-all range of surface temperature from 535° to 3050° R, inlet-air temperature from 535° to 1500° R, Reynolds number up to 500,000, exit Mach number up to 1, heat flux up to 150,000 Btu per hour per square foot, length-diameter ratio from 30 to 120, and three entrance configurations. Most of the data are for heat addition to the air; a few results are included for cooling of the air. The over-all range of surface-to-air temperature ratio was from 0.46 to 3.5.

Correlation of the measured average heat-transfer and friction coefficients with heat addition by conventional methods wherein the physical properties of the air were evaluated at the average air temperature resulted in considerable decreases in both the Nusselt number and the friction coefficient at constant Reynolds number in the turbulent region, as the ratio of surface temperature to air temperature was increased. The effect of surface-to-air temperature ratio was eliminated by evaluating the physical properties of air, including density, in the Reynolds number, the Nusselt number, and the friction coefficient at a temperature higher than the average air temperature.

Correlation of the heat-transfer coefficients was also affected by increases in the average air temperature, produced by increasing the inlet-air temperature, which resulted in a decrease in the Nusselt number. This effect of temperature level was reduced by using the smallest variation of thermal conductivity with temperature available in the literature and was eliminated when the thermal conductivity was arbitrarily assumed to vary as the square root of temperature.

INTRODUCTION

A large amount of data is available in the literature on forced-convection heat transfer from surfaces to fluids. Most of these data, however, have been obtained at relatively low surface temperatures and heat-flux densities, and do not extend into the range of high temperature and flux that is of interest in many current engineering applications. Inasmuch as convective heat transfer is a boundary-layer phenomenon, the severe temperature and velocity gradients in the fluid film adjacent to the surface (and attendant variation in fluid properties), which accompany heat transfer at high flux densities, make extrapolation of existing data for low flux densities uncertain. This possibility has been previously recognized; for example, in references 1 and 2 it is indicated that heat transfer and friction may depend on both surface and fluid temperatures.

An experimental investigation was undertaken at the NACA Lewis laboratory during 1948–50 to obtain heat-transfer and related pressure-drop information for a wide range of surface and fluid temperatures and heat flux. As part of the general program, an investigation was made with air flowing through smooth tubes. The effects of such variables as surface temperature, inlet-air temperature, and tube-entrance configuration on heat transfer and pressure drop have been investigated and are reported in references 3 to 6. The results of references 3 to 6 are summarized herein and, in addition, previously unpublished data showing the effect of tube length-diameter ratio and inlet-air temperature on heat-transfer and friction coefficients at high surface temperature and heat flux are presented. Most of the data are for heat addition to the air; however, a few previously unpublished results are included for heat extraction from the air.

APPARATUS

ARRANGEMENT

A schematic diagram of the equipment used in the investigation is shown in figure 1 (a). Compressed air was supplied through a pressure-regulating valve, cleaner, and surge tank to a second pressure-regulating valve where the flow rate was controlled. From this second valve, the air flowed through metering devices and a preheater into a mixing tank, which consisted of three concentric passages so arranged that the air made three passes through the tank before entering the test section. Baffles were provided in the central passage to insure thorough mixing of the air before it entered the test section. From the test section the air flowed through a second mixing tank and was discharged to the atmosphere. The test section, mixing tanks, and adjoining piping were thermally insulated.

[1] Supersedes NACA RM E7L31, "Heat Transfer from High-Temperature Surfaces to Fluids. I—Preliminary Investigation with Air in Inconel Tube with Rounded Entrance, Inside Diameter of 0.4 Inch, and Length of 24 Inches" by Leroy V. Humble, Warren H. Lowdermilk, and Milton Grele, 1948; NACA RM E8L03, "Heat Transfer from High-Temperature Surfaces to Fluids. II—Correlation of Heat-Transfer and Friction Data for Air Flowing in Inconel Tube with Rounded Entrance" by Warren H. Lowdermilk and Milton D. Grele, 1949; NACA RM E50E23, "Influence of Tube-Entrance Configuration on Average Heat-Transfer Coefficients and Friction Factors for Air Flowing in an Inconel Tube" by Warren H. Lowdermilk and Milton D. Grele, 1950; NACA RM E50H23, "Correlation of Forced-Convection Heat-Transfer Data for Air Flowing in Smooth Platinum Tube with Long-Approach Entrance at High Surface and Inlet-Air Temperatures" by Leland G. Desmon and Eldon W. Sams, 1950.

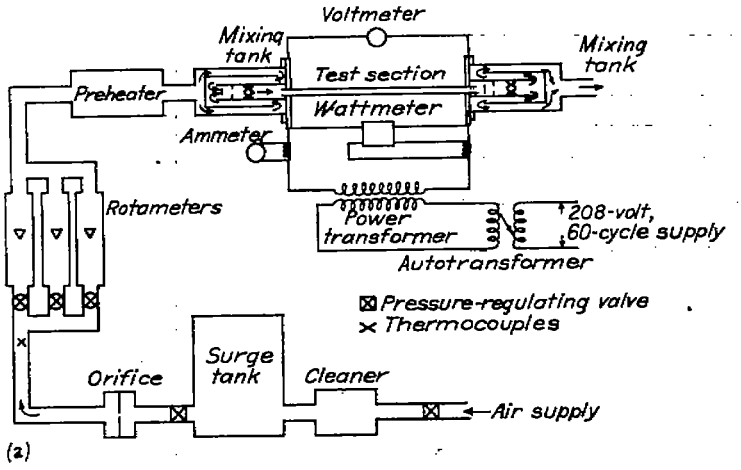

(a) Schematic diagram of setup.

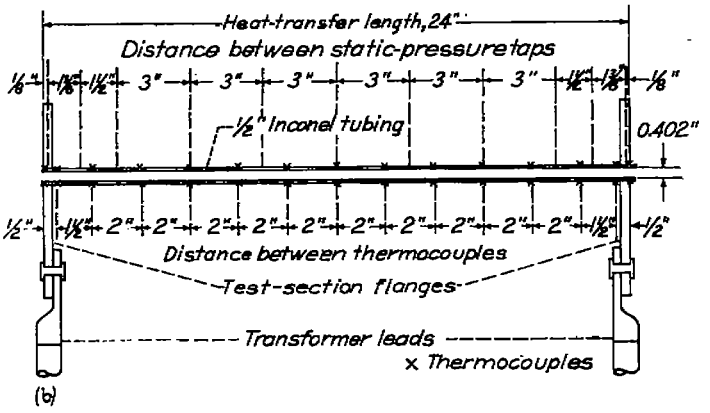

(b) Typical test section showing thermocouple and pressure-tap locations.

FIGURE 1.—Arrangement of apparatus for heating air.

The temperature of the air entering and leaving the test section was measured by thermocouples located downstream of the mixing baffles in the entrance and exit mixing tanks, respectively.

For the runs with heat addition to the air, electric power was supplied to the test section from a 208-volt, 60-cycle supply line through an autotransformer and a step-down power transformer. The low-voltage leads from the power transformer were connected to flanges on the test section by flexible copper cables. A voltmeter, an ammeter, and a wattmeter were provided to measure the electric-power input to the test section.

For the runs with heat extraction from the air, the electric-power supply was disconnected and the test section was surrounded with a water jacket. The warmed air from the preheater was cooled in the water-jacketed test section.

TEST SECTIONS

Most of the investigation was conducted using test sections fabricated from commercial Inconel tubing. The range of tube-wall temperature was extended beyond that attainable with Inconel by using one test section made of platinum (reference 6), which was installed in a separate setup similar to that shown in figure 1 (a). One of the test sections used

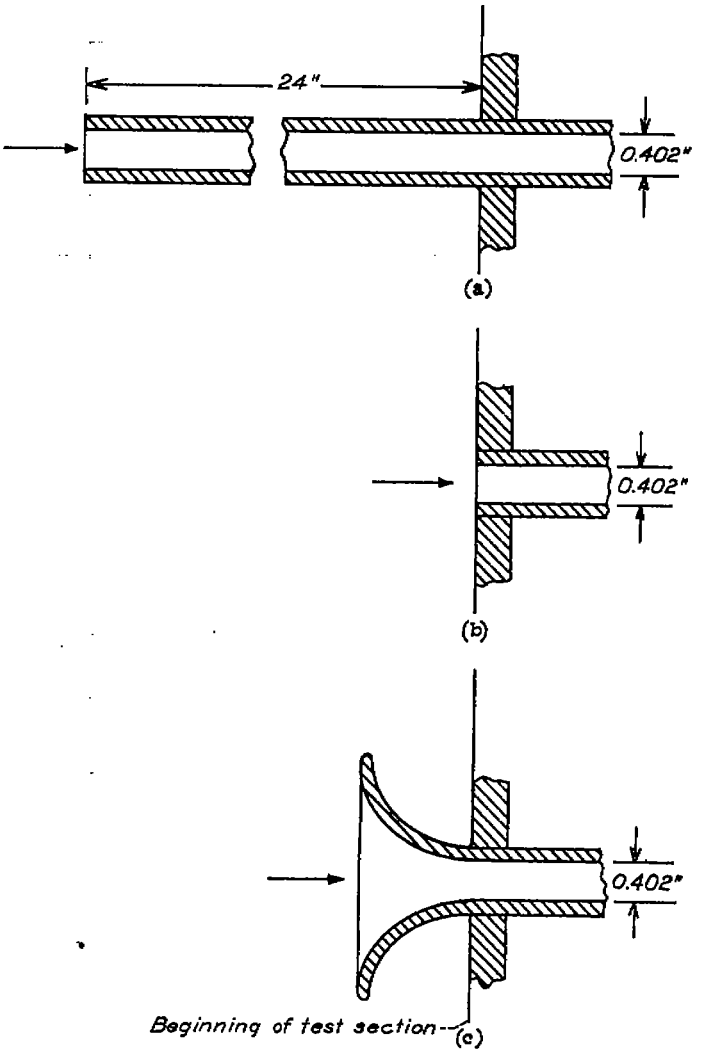

(a) Long approach.
(b) Right-angle edge.
(c) Bellmouth.

FIGURE 2.—Entrances to test sections.

for heating the air is illustrated schematically in figure 1 (b). Flanges were attached to both ends of the tube to provide electric contact with the power supply. The dimensions of the various tubes used as test sections in the investigation were as follows:

Tube material	Inside diameter (in.)	Outside diameter (in.)	Heat-transfer length (in.)	Length-diameter ratio
Inconel	0.402	0.500	12	30
Do	.402	.500	24	60
Do	.402	.500	48	120
Platinum	.525	.685	24	46

Outside-wall temperatures were measured at a number of stations along the tube by means of thermocouples and self-balancing indicating-type potentiometers. Chromel-alumel thermocouples were used with the Inconel test sections, and platinum—platinum-rhodium thermocouples, with the platinum test section. In general, at each station along the tube, two thermocouples were located diametrically opposite and

the average of the two temperatures was taken as the outside-wall temperature at the station. Static-pressure taps were located at intervals along each of the Inconel test sections.

Investigations were made with heat addition to the air using three types of entrance on the 24-inch Inconel tube (reference 5). The entrances, shown in figure 2, were (a) long approach, (b) right-angle edge, and (c) bellmouth.

The cooling data were obtained with an Inconel test section having a length-diameter ratio of 60 and a bellmouth entrance.

PROCEDURE

The following general procedure was used in obtaining the experimental data: For the heating runs, the inlet-air temperature was set at the desired value, the inlet-air pressure was adjusted to give the minimum desired flow rate (minimum Reynolds number), and the electric-power input was adjusted to give the desired tube-wall temperature. After equilibrium conditions had been attained, electric-power input, flow rate, temperatures, and pressures were recorded. The air flow and the power input were then increased in increments (to increase the Reynolds number while maintaining constant wall temperature) and data were recorded after each incremental increase. The foregoing procedure was repeated for a range of tube-wall temperature with each of the various test sections and entrance configurations.

For the cooling runs, the inlet-air pressure was adjusted to give the minimum desired air-flow rate at the desired inlet-air temperature. The water-flow rate in the water jacket was set at a constant value. After equilibrium conditions were obtained, the data were recorded as in the heating runs. The inlet-air pressure was then incrementally varied to cover a range of Reynolds number while maintaining constant inlet-air temperature. The foregoing procedure was repeated for a range of inlet-air temperature.

The over-all range of conditions for which data were obtained is summarized in the following table:

Reference	Tube material	Length-diameter ratio	Entrance type	Maximum bulk Reynolds number	Average tube-wall temperature (°R)	Inlet-air temperature (°R)	Maximum exit Mach number
3	Inconel	60	Bellmouth	250,000	680–1700	535	1.0
4	do	60	do	500,000	535–2050	535	1.0
5	do	60	Long approach, right angle	375,000	535–1960	535	1.0
6	Platinum	46	Long approach	320,000	980–3050	535–1160	0.6
(a)	Inconel	30	Bellmouth	390,000	535–1685	535	1.0
(a)	do	120	do	282,000	535–1850	535–1460	1.0
(a), (b)	do	60	do	250,000	535–585	535–1500	1.0

[a] Previously unpublished.
[b] Cooling data.

The over-all range of heat-flux density encountered in the investigation was from 500 to 150,000 Btu per hour per square foot of heat-transfer area.

213637—53——23

SYMBOLS

The following symbols are used in the report:

c_p	specific heat of air at constant pressure (Btu/(lb) (°F))
D	inside diameter of test section (ft)
f	average friction coefficient
f_f, f_s	modified average friction coefficient
G	mass velocity (mass flow per unit cross-sectional area) (lb/(hr) (sq ft))
g	acceleration due to gravity (4.17×10^8 ft/hr^2)
h	average heat-transfer coefficient (Btu/(hr) (sq ft) (°F))
k	thermal conductivity of air (Btu/(hr) (sq ft) (°F/ft))
k_t	thermal conductivity of test-section material (Btu/(hr) (sq ft) (°F/ft))
L	heat-transfer length of test section (ft)
P	absolute total or stagnation pressure (lb/(sq ft))
p	absolute static pressure (lb/(sq ft))
Δp	over-all static-pressure drop across test section (lb/(sq ft))
Δp_{fr}	friction static-pressure drop across test section (lb/(sq ft))
Q	rate of heat transfer to air (Btu/hr)
R	gas constant for air (53.35 ft-lb/(lb) (°F))
r	radius of test section (ft)
S	heat-transfer area of test section (sq ft)
T	total or stagnation temperature (°R)
T_b	average bulk temperature, defined by $(T_1+T_2)/2$, (°R)
T_f	average film temperature, defined by $(T_s+T_b)/2$, (°R)
$T_{0.75}$	average film temperature, defined by $T_b+0.75\ (T_s-T_b)$, (°R)
T_o	average outside-wall temperature of test section (°R)
T_s	average inside-wall (surface) temperature of test section (°R)
t	static temperature (°R)
V	velocity (ft/hr)
V_{av}	average velocity, defined by G/ρ_{av}, (ft/hr)
W	air flow (lb/hr)
x	distance from entrance of test section (ft)
γ	ratio of specific heats of air
μ	absolute viscosity of air (lb/(hr) (ft))
ρ	density of air (lb/(cu ft))
ρ_{av}	average density of air defined by $(p_1+p_2)/R\ (t_1+t_2)$, (lb/(cu ft))
$c_p\mu/k$	Prandtl number
GD/μ	Reynolds number
$\rho_f V_b D/\mu_f$, $\rho_{0.75} V_b D/\mu_{0.75}$, $\rho_s V_b D/\mu_s$	modified Reynolds number
hD/k	Nusselt number

Subscripts:

1	test-section entrance
2	test-section exit
i	inner surface of test section
o	outer surface of test section
b	bulk (when applied to properties, indicates evaluation at average bulk temperature T_b)
f	film (when applied to properties, indicates evaluation at average film temperature T_f)
0.75	film (when applied to properties, indicates evaluation at $T_{0.75}$)
s	surface (when applied to properties, indicates evaluation at average inside-wall temperature of test section T_s)

METHOD OF CALCULATION

Physical properties of air.—The physical properties of air used in the present investigation are shown in figure 3 as functions of temperature. The solid curves are from references 7 and 8, and are in agreement with the values of reference 9. The dashed curve for thermal conductivity is from reference 10. The dotted curve represents values of thermal conductivity assumed herein to vary as the square root of temperature and its use will be discussed in a subsequent section. The thermal conductivities from references 7 to 10 were extrapolated considerably beyond the range of experimental data in the reference reports and have been extrapolated still further in figure 3 to cover the temperature range of the present investigation. The upper temperature limits of the experimental data upon which values of thermal conductivity from references 7, 8, and 10 are based are 1050°, 1360°, and 1215° R, respectively.

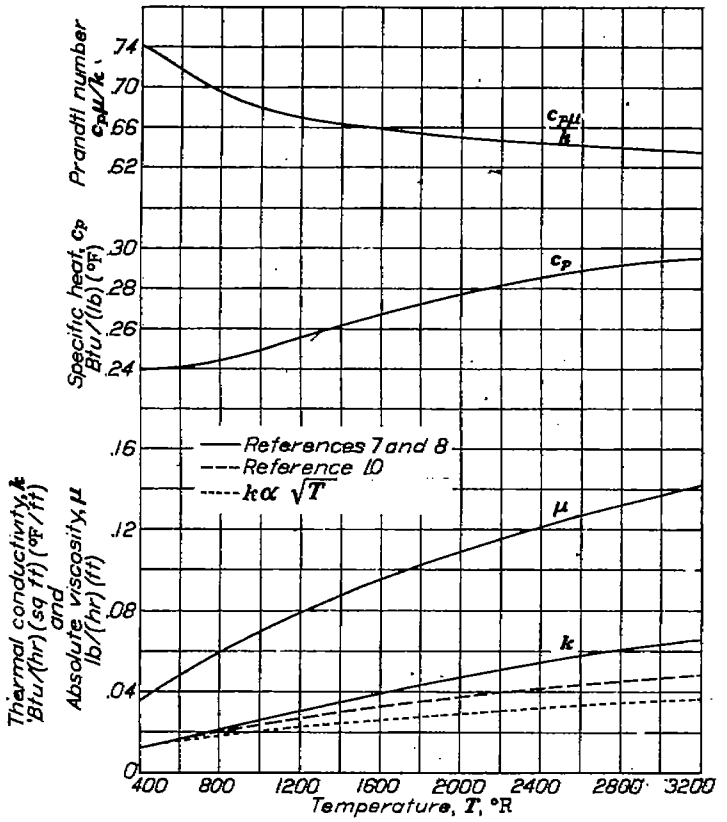

FIGURE 3.—Variation of thermal conductivity, absolute viscosity, specific heat, and Prandtl number of air with temperature.

Except where otherwise stated, the physical property data of references 7 and 8 are used in the present report.

Determination of surface temperature.—The average outside-wall temperature of the test section T_o was obtained by measuring the area under a curve of the temperature distribution (as obtained from thermocouple readings) along the heat-transfer length and dividing the area by this length.

For the heating runs, the average inside-wall (surface) temperature T_s was then calculated by the following equation (derived in reference 11):

$$T_s = T_o - \frac{Q}{2\pi L k_t (r_o^2 - r_i^2)} \left(r_o^2 \ln \frac{r_o}{r_i} - \frac{r_o^2 - r_i^2}{2} \right) \qquad (1)$$

In equation (1), the assumptions are made that heat is generated uniformly across the tube-wall thickness and that the heat flow from every point in the tube material is radially inward. For the present investigation, the radial temperature drop through the tube wall, calculated from equation (1), was very small compared with the difference between the average inside-wall and the air bulk temperature.

For the cooling runs, the thermocouples were imbedded in the test-section wall and were assumed to measure the inside-wall temperature, inasmuch as the calculated temperature drops through the wall were small.

Heat-transfer coefficients.—The average heat-transfer coefficient h was computed from the experimental data by the relation

$$h = \frac{W c_{p,b} (T_2 - T_1)}{S(T_s - T_b)} \qquad (2)$$

The use of the total air temperature T_b instead of adiabatic wall temperature was considered justified because the difference between these temperatures was small compared with the difference between the average surface and air (or adiabatic wall) temperatures.

Correlation of the average heat-transfer coefficients with the pertinent variables is discussed in the section **RESULTS AND DISCUSSION.**

Friction coefficients.—Friction data were obtained with and without heat transfer. Average friction coefficients were calculated from the experimental pressure-drop data as follows: The friction pressure drop was obtained by subtracting the calculated momentum pressure drop from the measured static-pressure drop across the test section. Thus

$$\Delta p_{fr} = \Delta p - \frac{G}{g}(V_2 - V_1) = \Delta p - \frac{G^2 R}{g}\left(\frac{t_2}{p_2} - \frac{t_1}{p_1}\right) \qquad (3)$$

where t_1 and t_2, the absolute static temperatures at entrance and exit of the test section, respectively, were, in general, calculated from the measured values of air flow, static pressure, and total temperature by the following equation, which is obtained by combining the perfect gas law, the equation of continuity, and the energy equation:

$$t=-\frac{\gamma g}{(\gamma-1)R}\left(\frac{p}{G}\right)^2+\sqrt{\left[\frac{\gamma g}{(\gamma-1)R}\left(\frac{p}{G}\right)^2\right]^2+2T\frac{\gamma g}{(\gamma-1)R}\left(\frac{p}{G}\right)^2} \tag{4}$$

For the bellmouth entrance, it was found that the entrance static temperature t_1 could be represented with sufficient accuracy by the relation

$$t_1=T_1\left(\frac{p_1}{P_1}\right)^{\frac{\gamma-1}{\gamma}} \tag{5}$$

In equation (5) the total pressure at the test-section entrance P_1 was assumed to be equal to the static pressure in the entrance mixing tank, where the velocity was negligible.

Average friction coefficients were calculated by dividing the friction pressure drop by four times the length-diameter ratio of the tube times a dynamic pressure. The density in the dynamic pressure was computed in three ways, resulting in three definitions of friction coefficient.

The first of these friction coefficients was based on a density evaluated at the average static pressure and temperature of the air in the tube; thus

$$f=\frac{\Delta p_{fr}}{4\frac{L}{D}\frac{\rho_{as}V_{as}^2}{2g}}=\frac{g\rho_{as}\Delta p_{fr}}{2\frac{L}{D}G^2} \tag{6}$$

where

$$\rho_{as}=\frac{1}{R}\left(\frac{p_1+p_2}{t_1+t_2}\right) \tag{7}$$

In the other two definitions of friction coefficient, the density was evaluated at the film temperature T_f and at the average surface temperature T_s, resulting in equations (8) and (9), respectively:

$$f_f=\frac{\Delta p_{fr}}{4\frac{L}{D}\frac{\rho_f V_{as}^2}{2g}}=\left(\frac{\rho_{as}}{\rho_f}\right)f=\left(\frac{2T_f}{t_1+t_2}\right)f \tag{8}$$

$$f_s=\frac{\Delta p_{fr}}{4\frac{L}{D}\frac{\rho_s V_{as}^2}{2g}}=\left(\frac{\rho_{as}}{\rho_s}\right)f=\left(\frac{2T_s}{t_1+t_2}\right)f \tag{9}$$

Correlation of the friction data is discussed in the following section.

RESULTS AND DISCUSSION

AXIAL WALL-TEMPERATURE DISTRIBUTIONS

Representative axial wall-temperature distributions obtained with heat addition to the air in an Inconel tube having a length-diameter ratio of 60 and a bellmouth entrance are shown in figure 4. The outside-wall temperature is plotted against the ratio of the distance from the tube entrance to the heat-transfer length x/L for five different rates of heat transfer to the air. The rate of heat transfer to the air, the air flow, the average inside tube-wall temperature, and the temperature rise of the air are tabulated.

The wall temperature increases almost linearly over the major portion of the tube length, and the slope of this part of the curve increases with an increase in rate of heat input. The large axial-temperature gradients at the entrance and exit of the test section are the result of conduction losses through the electric connector flanges and cables.

The curves in figure 4 are typical; similar trends were obtained with other entrances and for other length-diameter ratios.

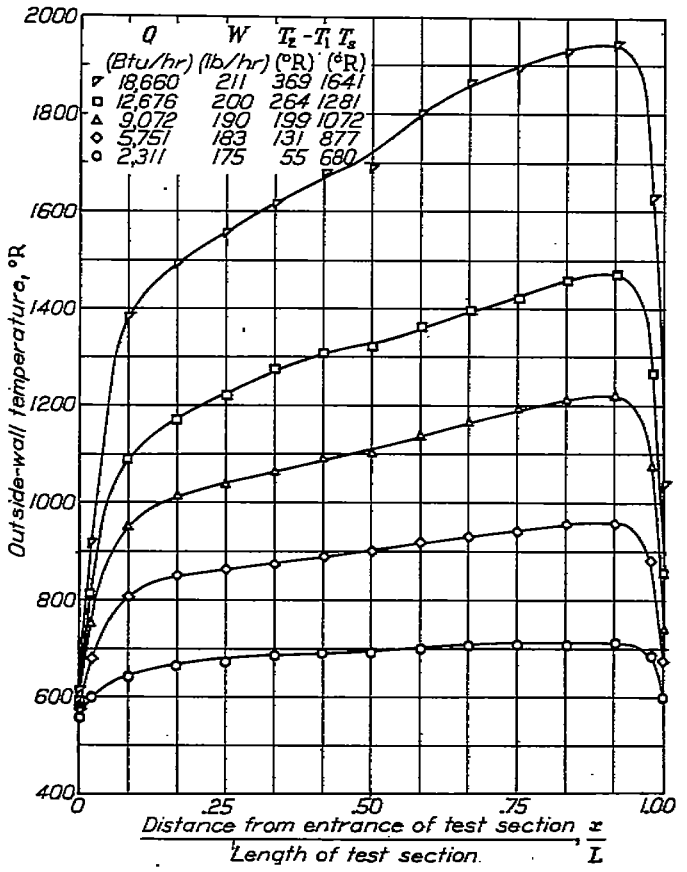

FIGURE 4.—Representative outside-wall temperature distribution for various amounts of heat input to air. Reynolds number, approximately 140,000; Inconel tube; length-diameter ratio, 60; bellmouth entrance; inlet-air temperature, 535° R.

CORRELATION OF HEAT-TRANSFER COEFFICIENTS

Conventional correlation based on average air temperature.—Forced-convection, turbulent-flow, heat-transfer coefficients are generally correlated with other pertinent variables by means of the familiar relation in which Nusselt number divided by Prandtl number to a power (generally 0.4) $\frac{hD}{k}\Big/\left(\frac{c_p\mu}{k}\right)^{0.4}$ is plotted against Reynolds number GD/μ, and in which the physical properties of the fluid (specific heat, viscosity, and thermal conductivity) are usually eval-

uated at the average fluid temperature. Results obtained by heating air flowing through an Inconel tube having a length-diameter ratio of 60 and a bellmouth entrance (reference 4) are plotted in this manner in figure 5 (a). The data shown are for an inlet-air total temperature of 535° R and cover a range of Reynolds number from about 7000 to 500,000. Included for comparison is the average line obtained by McAdams (reference 2) from correlation of the results of various investigators. The equation corresponding to this reference line is

$$\frac{hD}{k_b}=0.023\left(\frac{GD}{\mu_b}\right)^{0.8}\left(\frac{c_{p,b}\mu_b}{k_b}\right)^{0.4} \qquad (10)$$

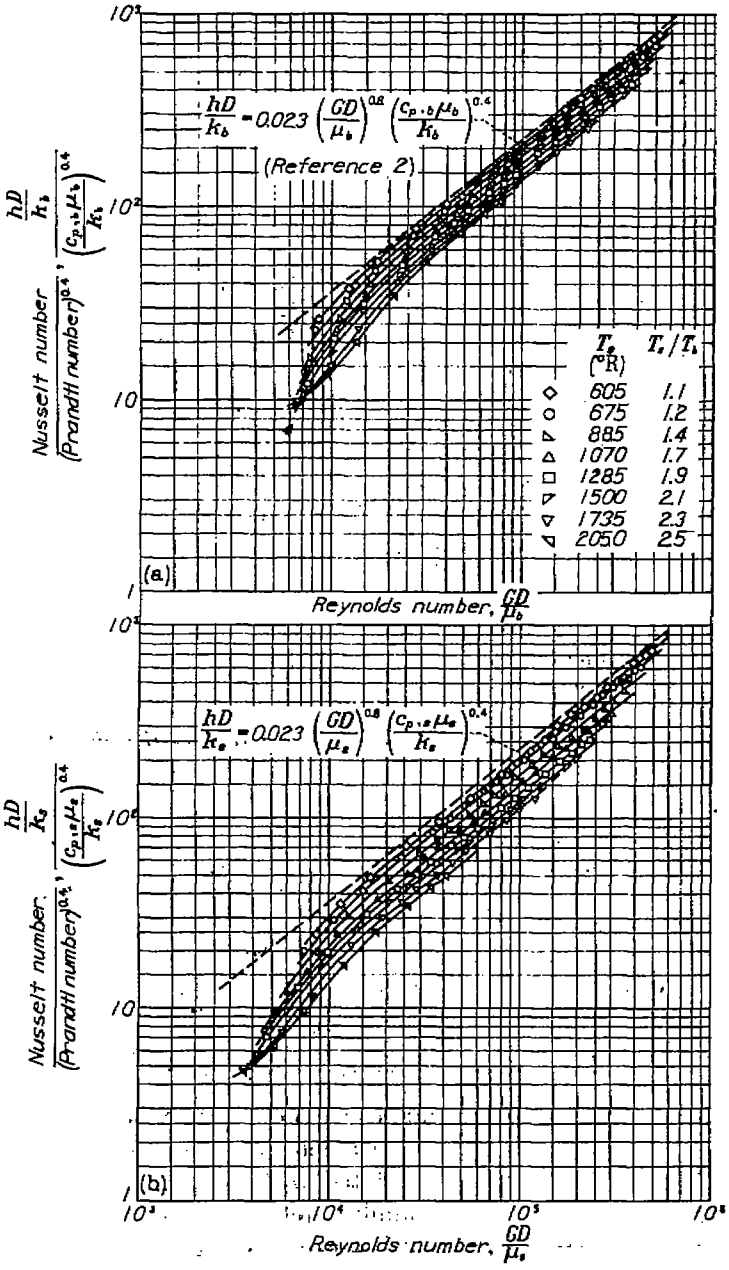

(a) Physical properties of air evaluated at average bulk temperature.
(b) Physical properties of air evaluated at average surface temperature.

FIGURE 5.—Conventional methods of correlating heat-transfer coefficients. Inconel tube; length-diameter ratio, 60; bellmouth entrance; inlet-air temperature, 535° R.

A family of parallel lines representing the various surface-to-air temperature ratios and having slopes of about 0.8 at Reynolds numbers above approximately 25,000 is obtained.

The data for low surface temperatures (T_s, 605° R) are in reasonable agreement with the reference line; however, as the surface temperature is raised the data fall progressively below the reference line. For example, at a Reynolds number of 70,000, an increase in T_s/T_b from 1.1 to 2.5 (corresponding to an increase in surface temperature from 605° to 2050° R) results in a decrease in the ordinate parameter of about 38 percent. Inasmuch as the corresponding change in Prandtl number to the 0.4 power is small, about the same percentage decrease occurs in Nusselt number.

The results shown in figure 5 (a) are typical of those obtained with other entrance configurations and length-diameter ratios.

Conventional correlation based on surface temperature.—The heat-transfer data of figure 5 (a) are replotted in figure 5 (b), wherein the physical properties of the air are evaluated at the average inside-wall temperature T_s. The line representing equation (10), but with the physical properties evaluated at T_s, is included for comparison. The data again show a separation with surface temperature level, which in this case is greater than when the properties are evaluated at the bulk temperature. The use of any temperature between these extremes would, of course, cause an intermediate amount of separation of the data.

In references 1 and 12, heat-transfer coefficients were predicted for fully developed flow of fluids having a Prandtl number of 1.0 in smooth tubes. The analyses took into consideration the radial variation of fluid properties and indicated an effect of surface-to-fluid temperature ratio analogous to that shown in figure 5.

Effect of surface-to-fluid temperature ratio.—The magnitude of the effect on the heat-transfer correlations of surface-to-fluid temperature ratios greater than 1.0 is illustrated more clearly in figure 6. Lines are shown for which the air properties are evaluated at bulk temperature T_b, film temperature T_f, and surface temperature T_s. The lines corresponding to evaluation of properties at T_b and T_s are cross plots of the data at a Reynolds number of 100,000 from figures 5 (a) and 5 (b), respectively. The line corresponding to evaluation of air properties at T_f was obtained from a plot similar to those of figure 5.

A series of straight lines is obtained, which intersect at T_s/T_b of 1.0, at which point the ordinate parameter has the value predicted by equation (10). The lines have increasingly greater negative slopes as the temperature at which the fluid properties are evaluated is increased. For example, an increase in T_s/T_b from 1.0 to 2.5 results in a decrease in the ordinate parameter of about 40 percent when the properties are evaluated at T_b, of 48 percent when evaluated at T_f, and of 54 percent when evaluated at T_s.

Appreciable error can be made (fig. 6) if conventional heat-transfer correlation equations are used to compute heat-transfer coefficients for surface-to-fluid temperature ratios appreciably greater than 1.0.

Modified correlation based on surface temperature.—The slope of the line in figure 6 corresponding to evaluation of the fluid properties at T_s is -0.8. The ordinate in this case is $(hD/k_s)/(c_{p,s}\mu_s/k_s)^{0.4}$ and the corresponding Reynolds number is defined by GD/μ_s. Inasmuch as at $T_s/T_b=1.0$ equation (10) applies, it might be expected that the effect of T_s/T_b could be eliminated by incorporating the term $(T_b/T_s)^{0.8}$ in equation (10) with the properties evaluated at T_s. Thus

$$\frac{hD}{k_s}=0.023\left(\frac{GD}{\mu_s}\right)^{0.8}\left(\frac{T_b}{T_s}\right)^{0.8}\left(\frac{c_{p,s}\mu_s}{k_s}\right)^{0.4} \tag{11}$$

If the difference between total and static temperatures is neglected,

$$\frac{T_b}{T_s}=\frac{\rho_s}{\rho_b} \tag{12}$$

and the following relation is obtained by letting $G=\rho_b V_b$:

$$\left(\frac{GD}{\mu_s}\right)\left(\frac{T_b}{T_s}\right)=\frac{\rho_s V_b D}{\mu_s} \tag{13}$$

Equation (13) defines a modified form of Reynolds number in which the conventional mass velocity G is replaced by the product of air density evaluated at the average surface temperature ρ_s and air velocity evaluated at the average bulk temperature V_b. Substituting equation (13) in equation (11) gives

$$\frac{hD}{k_s}=0.023\left(\frac{\rho_s V_b D}{\mu_s}\right)^{0.8}\left(\frac{c_{p,s}\mu_s}{k_s}\right)^{0.4} \tag{14}$$

The data of figure 5 are replotted in figure 7. Nusselt number divided by Prandtl number to the 0.4 power is plotted against the modified Reynolds number $\rho_s V_b D/\mu_s$.

The use of the modified Reynolds number eliminates the trends with respect to surface-to-bulk temperature ratio, so that for the range of surface temperature and Reynolds number shown the data can be represented with good accuracy by a single line. For modified Reynolds numbers above about 10,000, the data can be represented very well by equation (14).

Effect of entrance configuration.—Heating data obtained with an Inconel tube having a length-diameter ratio of 60 and both long-approach and right-angle-edge entrances are shown in figure 8. The coordinates are the same as in figure 7, and the line representing the data of figure 7 (bellmouth entrance) is included in the figure.

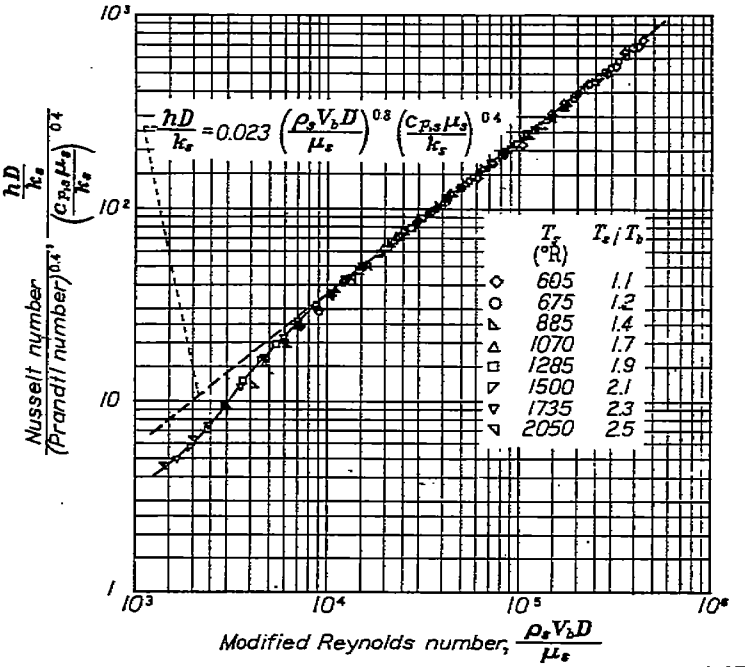

FIGURE 7.—Modified method of correlating heat-transfer coefficients. Inconel tube; length-diameter ratio, 60; bellmouth entrance; inlet-air temperature, 535° R; physical properties of air evaluated at surface temperature.

The long-approach and bellmouth entrances tend to provide fully developed and uniform velocity profiles, respectively, at the inlet to the test section. The right-angle-edge entrance is typical of most tube-type heat exchangers.

As shown in figure 8, the data obtained with the long-approach and right-angle-edge entrances can be represented with good accuracy by the line which best fitted the data for the bellmouth entrance shown in figure 7. It may be concluded that the average heat-transfer coefficient is negligibly affected by the entrance configurations investigated, at least for length-diameter ratios of the order of 60 or greater.

Effect of length-diameter ratio.—Heating data obtained with Inconel tubes having length-diameter ratios of 30 and 120 and with a platinum tube having a length-diameter ratio of 46 (reference 6) are shown in figure 9 (a). The coordinates are the same as in figures 7 and 8 and the line (shown solid) representing the data of figures 7 and 8, which

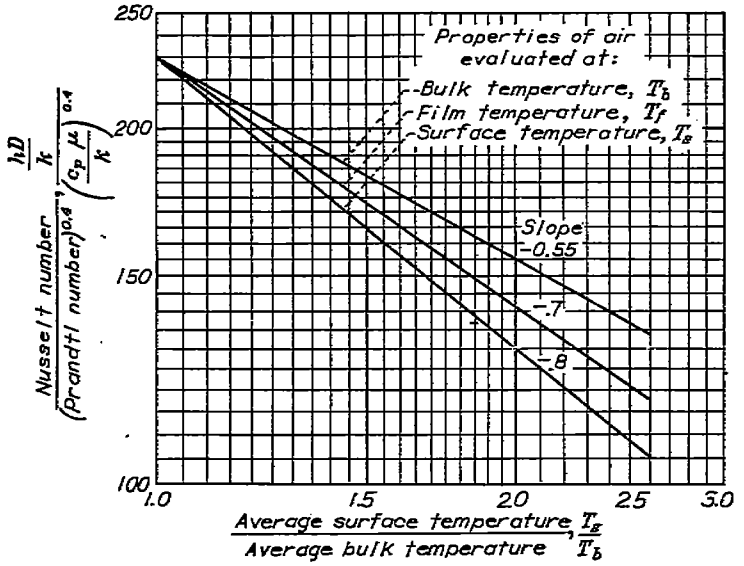

FIGURE 6.—Variation of Nusselt number divided by Prandtl number to 0.4 power with ratio of surface-to-bulk temperature using conventional methods of correlating heat-transfer coefficients. Reynolds number, 100,000; Inconel tube; length-diameter ratio, 60; bellmouth entrance; inlet-air temperature, 535° R.

are for a length-diameter ratio of 60, is included. The Inconel tubes had bellmouth entrances, and the platinum tube had a long-approach entrance; however, as indicated in figure 8, the effect of entrance configuration is negligible.

A small trend with respect to length-diameter ratio is evident in the turbulent region. The data for length-diameter ratios less than 60 tend to fall parallel to, but above, the reference line, whereas the data for a length-diameter ratio of 120 fall below the line. This effect of length-

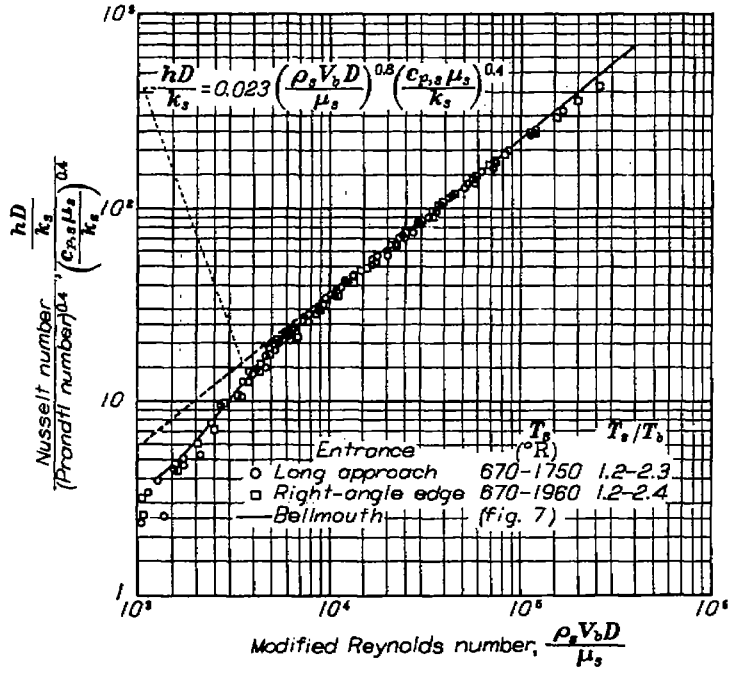

FIGURE 8.—Effect of entrance configuration using modified method of correlating heat-transfer coefficients. Inconel tube; length-diameter ratio, 60; inlet-air temperature, 535° R; physical properties of air evaluated at surface temperature.

diameter ratio has been observed by other investigators (see, for example, references 1 and 13) and was accounted for by including a power function of the length-diameter ratio in the general correlation equation. The exponent 0.054 is quoted in reference 1 and the value 0.1 is quoted in reference 13. The exponent 0.1 applies best for the present data and accordingly the data of figures 7 and 9 (a), corrected for the effect of length-diameter ratio, are replotted in figure 9 (b).

The correction for length-diameter ratio appreciably improves the correlation for modified Reynolds numbers above approximately 10,000, and in this region the data can be represented by the following equation:

$$\frac{hD}{k_s}=0.034\left(\frac{\rho_s V_b D}{\mu_s}\right)^{0.8}\left(\frac{c_{p,s}\mu_s}{k_s}\right)^{0.4}\left(\frac{L}{D}\right)^{-0.1} \qquad (15)$$

The constant 0.034 is 0.023 (equation (14)) multiplied by $60^{0.1}$, where 60 is the length-diameter ratio of the tube used in obtaining the data upon which equation (14) is based.

The data for modified Reynolds numbers below about 10,000 show a trend with respect to length-diameter ratio and cannot be represented by a single line.

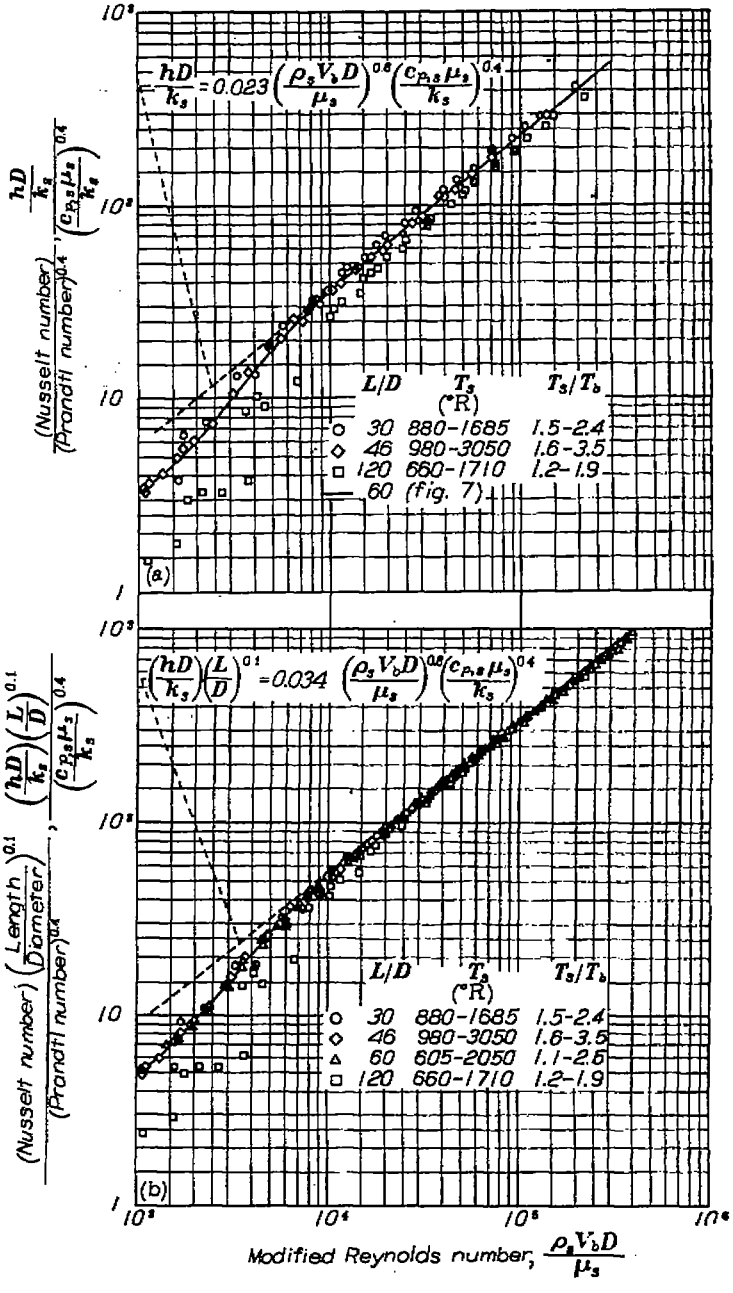

(a) Uncorrected for effect of length-diameter ratio.
(b) Corrected for effect of length-diameter ratio.

FIGURE 9.—Effect of ratio of length to diameter using modified method of correlating heat transfer coefficients. Inconel and platinum tubes; inlet-air temperature, 535° R; physical properties of air evaluated at surface temperature.

The data shown in figure 9 for the platinum tube (L/D, 46) were obtained for surface temperatures up to 3050° R and surface-to-air temperature ratios up to 3.5; it is of interest that, for this extended range of temperature, the data are correlated with negligible scatter by use of the modified Reynolds number.

Effect of air temperature.—The data presented thus far were obtained with an inlet-air temperature of about 535° R. A wide range of surface temperature and corresponding surface-to-air temperature ratio was investigated. In order to determine whether the correlation applied for a wider

range of air temperature, tests were made in which the inlet-air temperature, and hence average air temperature, was varied. The results are shown in figure 10.

Inspection of figure 10 indicates that the ordinate parameter decreases as the inlet-air temperature and the corresponding average air temperature increase. For example, in figure 10 (a), at a Reynolds number of approximately 100,000 and a surface temperature of approximately 1800° R, an increase in inlet-air temperature from 535° to 1460° R (with a corresponding decrease in T_s/T_b from 1.9 to 1.2) results in a reduction in the ordinate parameter of about 24 percent. The ordinate parameter would decrease further if the inlet temperature were increased until T_s/T_b was approximately 1.0. At constant values of T_s/T_b, the ordinate parameter varies approximately as temperature to the −0.2 power.

As much as one-fourth of the observed separation of the data with temperature level may be caused by experimental error in measuring air temperature at the high temperature levels. Inasmuch as there is a considerable variation in the reported values of thermal conductivity at high temperature, as is evident in figure 3, the effect may be partly or entirely the result of using improperly extrapolated values of thermal conductivity.

The values of conductivity from references 7 and 8, which have been used thus far in correlating the present data, vary approximately as the 0.85 power of the absolute temperature. The values from reference 10 vary approximately as the 0.73 power of the temperature. Inasmuch as the ordinate parameter of figure 10 varies inversely as conductivity to the 0.6 power, the conductivity would have to vary as temperature to the 0.85 power minus 0.2 divided by 0.6, or to the 0.5 power, in order to completely eliminate the effect of temperature level in figures 10 (a) and (b).

Inspection of figures 5 and 6 indicates that the use of smaller values of thermal conductivity at high temperatures in correlation of the data would also result in a decrease of the effect of surface-to-air temperature ratio, so that correlation of the data according to equation (15), in which the fluid physical properties and density are evaluated at the surface temperature, would result in an overcorrection of the data with increasing values of surface-to-air temperature ratio. A relation of the form of equation (15) can, however, be used for correlation of the data by evaluating the fluid physical properties and density at a reference temperature lower than the surface temperature. For example, if conductivity is assumed to vary as temperature to the 0.73 power, the effect of surface-to-air temperature ratio can be decreased by using a reference temperature $T_{0.75}$ midway between T_f and T_s. If conductivity is assumed to vary as the square root of temperature, the effect can be eliminated by using the film temperature T_f as the reference temperature.

In order to illustrate the effect of using smaller values of thermal conductivity at high temperatures, the data of

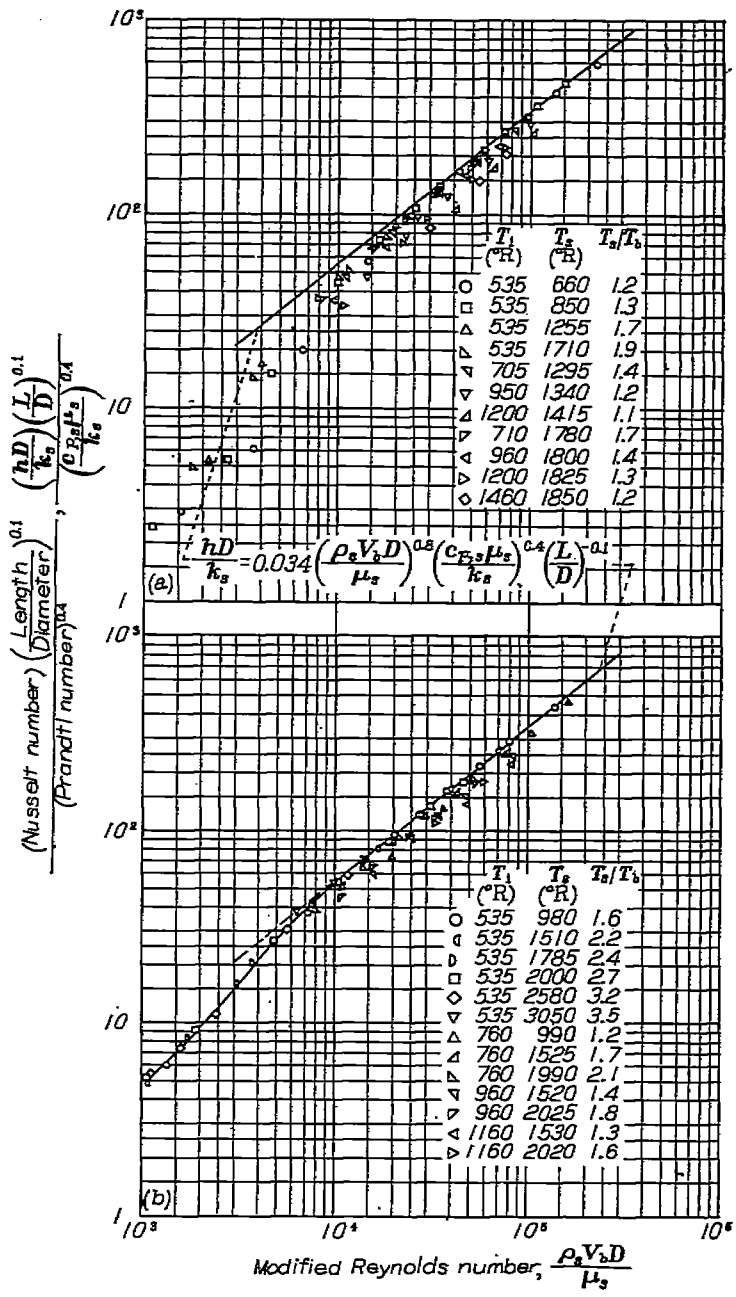

(a) Physical properties of air evaluated at surface temperature; thermal conductivity proportional to $T^{0.85}$; Inconel tube; length-diameter ratio, 120.

(b) Physical properties of air evaluated at surface temperature; thermal conductivity proportional to $T^{0.55}$; platinum tube; length-diameter ratio, 46.

FIGURE 10.—Effect of inlet-air temperature using modified method of correlating heat-transfer coefficients.

figure 10 (a) are replotted in figure 10 (c) using the conductivity data of reference 10, and with the physical properties and density evaluated at the film temperature $T_{0.75}$. The line representing equation (15), which for the lower reference temperature becomes

$$\frac{hD}{k_{0.75}}=0.034\left(\frac{\rho_{0.75}V_bD}{\mu_{0.75}}\right)^{0.8}\left(\frac{c_{p,0.75}\mu_{0.75}}{k_{0.75}}\right)^{0.4}\left(\frac{L}{D}\right)^{-0.1} \quad (15a)$$

is included for comparison.

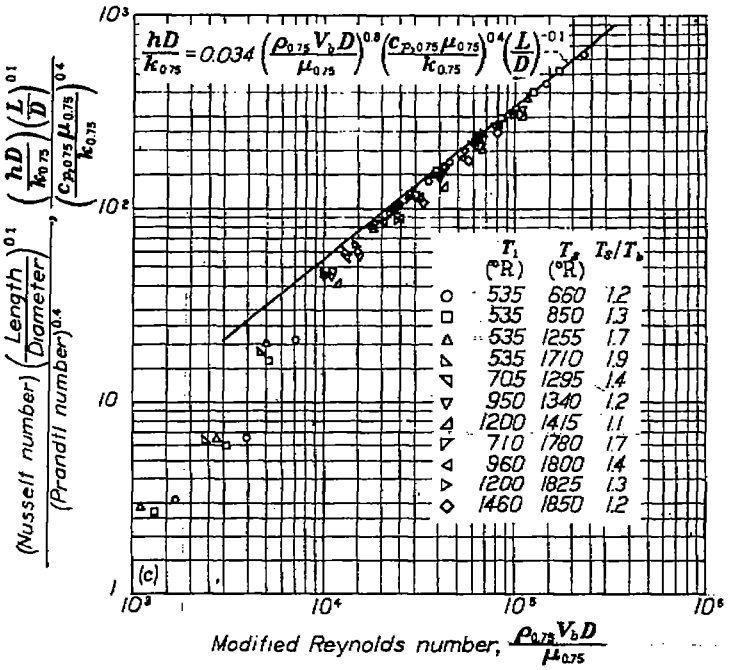

(c) Physical properties of air evaluated at film temperature $T_{0.75}$; thermal conductivity proportional to $T^{0.75}$; Inconel tube.

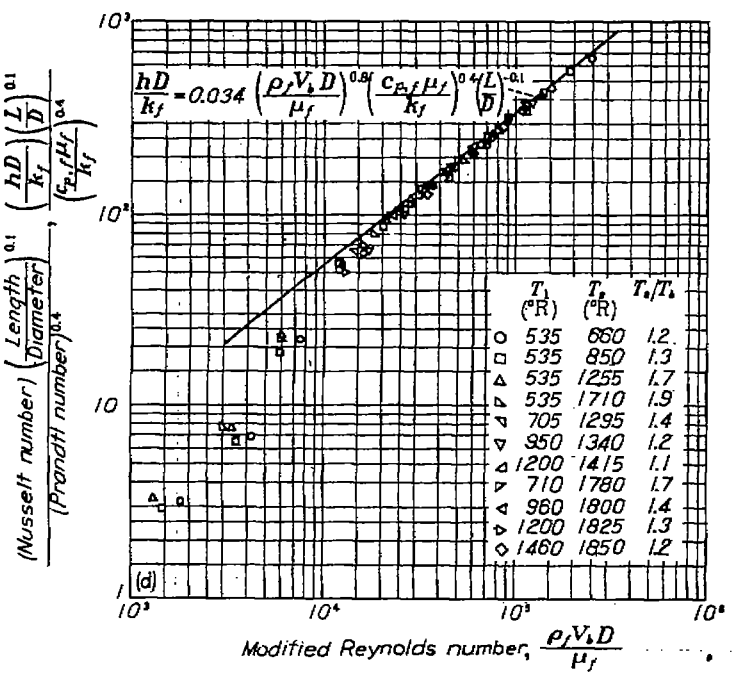

(d) Physical properties of air evaluated at film temperature T_f; thermal conductivity proportional to $\sqrt{T}$; Inconel tube.

FIGURE 10.—Concluded. Effect of inlet-air temperature using modified method of correlating heat-transfer coefficients.

For an inlet-air temperature of 1460° R, a surface temperature of 1850° R, and a Reynolds number of 85,000, the ordinate parameter is about 15 percent below the reference line. Comparison of figures 10 (a) and 10 (c) indicates that the use of the lower values of conductivity from reference 10 reduces the effect of temperature level by approximately one-half, or for constant values of T_s/T_b, the ordinate parameter varies as temperature to the −0.1 power.

The data of figure 10 (b), although not shown, would fall within the total separation of the data in figure 10 (c).

Figure 10 (d) is included to illustrate the effect of using still lower values of thermal conductivity at high temperatures. The data are the same as in figures 10 (a) and 10 (c), but in figure 10 (d) the conductivity is assumed to vary as the square root of temperature and the physical properties and density are evaluated at the film temperature T_f. The line representing equation (15), which for the reference film temperature T_f becomes

$$\frac{hD}{k_f} = 0.034 \left(\frac{\rho_f V_b D}{\mu_f}\right)^{0.8} \left(\frac{c_{p,f}\mu_f}{k_f}\right)^{0.4} \left(\frac{L}{D}\right)^{-0.1} \qquad (15b)$$

is included for comparison.

In figure 10 (d) it is indicated that both the effects of air temperature and surface-to-air temperature ratio are eliminated by use of the assumed conductivity-temperature relation and by evaluation of the physical properties and density at the film temperature. The data can be represented with good accuracy by equation (15b).

No justification of the arbitrarily assumed conductivity-temperature relation shown in figure 3 can be given other than that it results in the best correlation of the data reported herein.

Effect of heat extraction.—In reference 12, it is predicted that with heat extraction from the air the Nusselt number would increase as the heat-flux density increases, or as the surface-to-air temperature ratio decreases. It was further found that the effect could be eliminated by evaluating the physical properties and density at a reference temperature midway between T_b and T_s.

Tests were conducted to determine whether or not the effect of T_s/T_b on correlation of heat-transfer coefficients was the same for heat extraction as for heat addition. These results were obtained with an Inconel tube having a length-diameter ratio of 60 and a bellmouth entrance for a range of T_s/T_b from 0.46 to 0.82. The data are correlated in the conventional manner in figure 11 using thermal conductivities from references 7 and 8 with the physical properties evaluated at the average temperature T_b. Included is the line representing equation (10) modified for variation in L/D, which becomes

$$\frac{hD}{k_b} = 0.034 \left(\frac{GD}{\mu_b}\right)^{0.8} \left(\frac{c_{p,b}\mu_b}{k_b}\right)^{0.4} \left(\frac{L}{D}\right)^{-0.1} \qquad (16)$$

The effect of a decrease in T_s/T_b from 0.82 to 0.46 on the correlation of the data is negligible, and the data can be adequately represented by equation (16).

The data in figure 11 do not necessarily show that no effect of T_s/T_b exists for cooling inasmuch as the use of a smaller variation of conductivity with temperature would result in an increase in Nusselt number for a decrease in T_s/T_b and hence introduce an effect of T_s/T_b into the data.

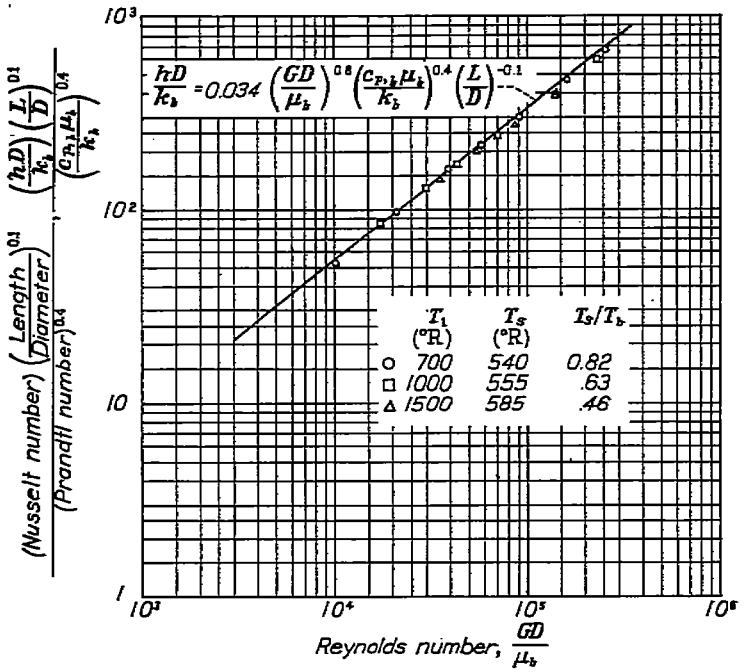

FIGURE 11.—Conventional method of correlating heat-transfer coefficients with heat e xtrac tion from air. Inconel tube; length-diameter ratio, 60; bellmouth entrance.

The effects of using smaller variations of conductivity are shown in figures 12 (a) and 12 (b) with the data based on the conductivity data of reference 10 and on the assumption that conductivity varies as the square root of temperature, respectively. In figure 12 (a), the data are correlated according to equation (15a) for heat addition. A considerable overcorrection for the effects of T_s/T_b is obtained, which indicates that the effect of T_s/T_b for cooling is smaller than that obtained for heating. In figure 12 (b), however, where the data are correlated according to equation (15b) for heat addition, the separation of the data is very small, indicating that for the assumption that conductivity varies as the square root of temperature the effect of T_s/T_b is the same for both the heating and cooling data, and that both the cooling and the heating data can be represented by equation (15b).

Summary plots of heat-transfer data.—Heat-transfer data have been shown for a range of Reynolds number, surface temperature, inlet-air temperature, entrance configuration, and length-diameter ratio, and for heating and cooling of the air. The results are summarized in figure 13, which shows on single plots data from previous figures, which include all the foregoing variables.

The data are correlated in figure 13 (a) by the modified method using the thermal conductivity data of references 7 and 8 with the physical properties and density evaluated at T_s. The line representing equation (15) is included for comparison. As previously shown, all the heating data obtained with an inlet-air temperature of 535° R regardless of length-diameter ratio, surface temperature, or entrance configuration can be represented with good accuracy by the

213637—53——24

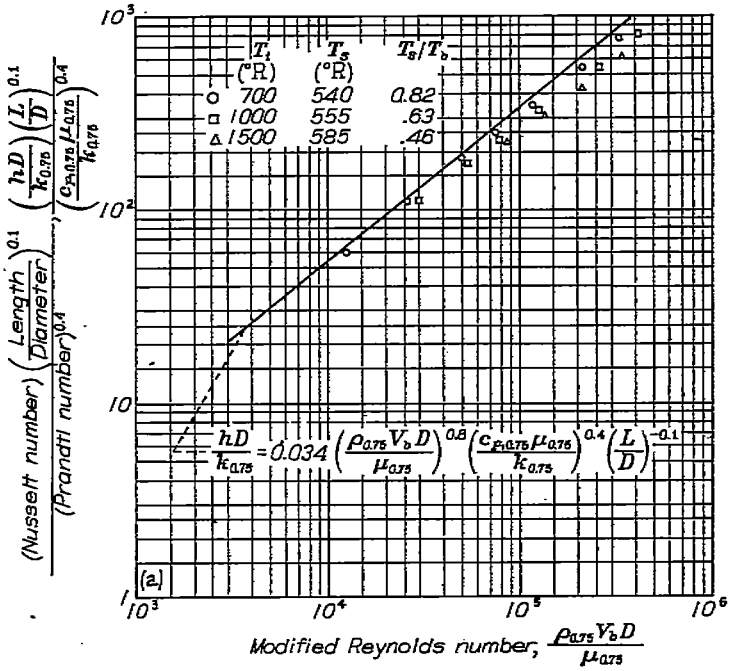

(a) Physical properties of air evaluated at film temperature $T_{s,75}$; thermal conductivity proportional to $T^{0.75}$.

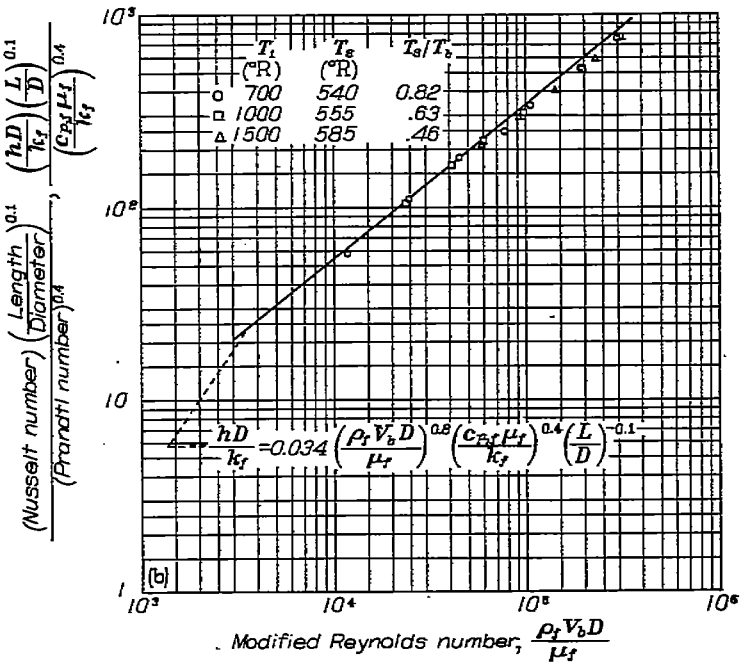

(b) Physical properties of air evaluated at film temperature T_f; thermal conductivity proportional to $\sqrt{T}$.

FIGURE 12.—Modified method of correlating heat-transfer coefficients with heat extraction from air.

reference line. The high inlet-air temperature data and the cooling data fall below the reference line, so that equation (15) does not apply with desirable accuracy for all the conditions investigated.

The data of figure 13 (a) are replotted in figure 13 (b) using the thermal conductivity data from reference 10, and with the physical properties and density evaluated at $T_{0.75}$.

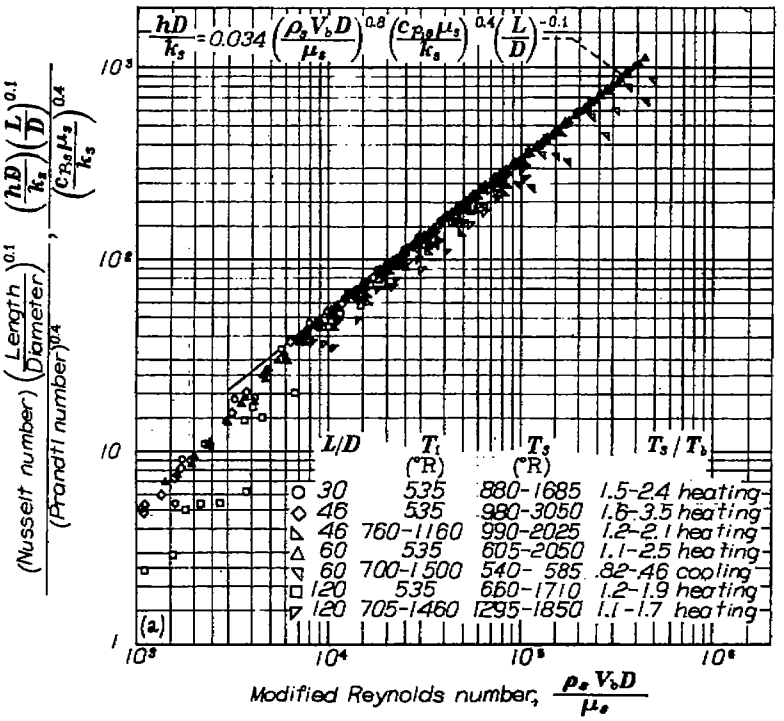

(a) Physical properties of air evaluated at surface temperature T_s; thermal conductivity proportional to $T^{0.68}$.

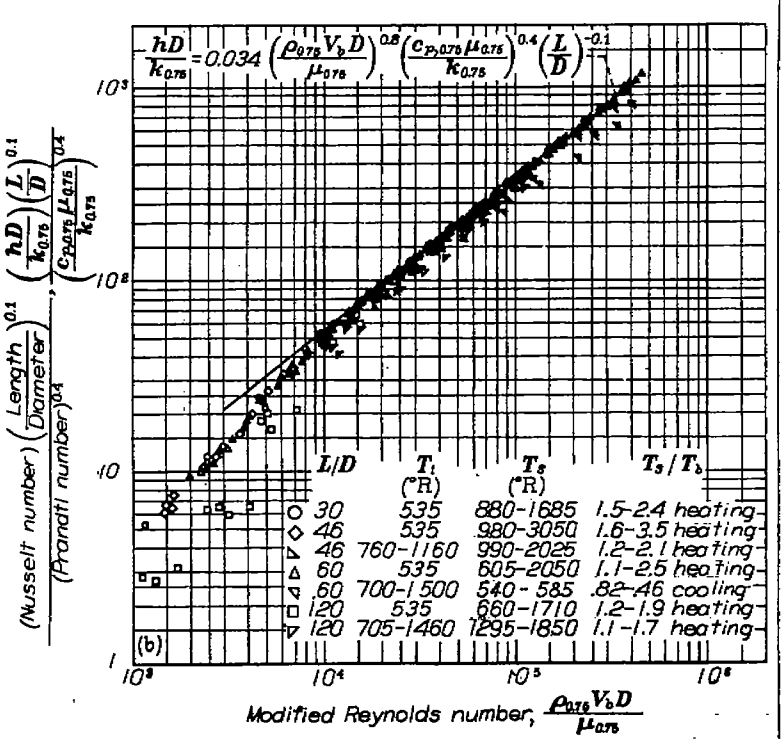

(b) Physical properties of air evaluated at film temperature $T_{0.75}$; thermal conductivity proportional to $T^{0.75}$.

FIGURE 13.—Summary plot of experimental data using modified method of correlating heat-transfer coefficients.

The line representing equation (15a) is included. Trends with temperature level and with T_s/T_b are reduced compared with figure 13 (a). The high inlet-air temperature data and the cooling data again deviate farthest from the reference line.

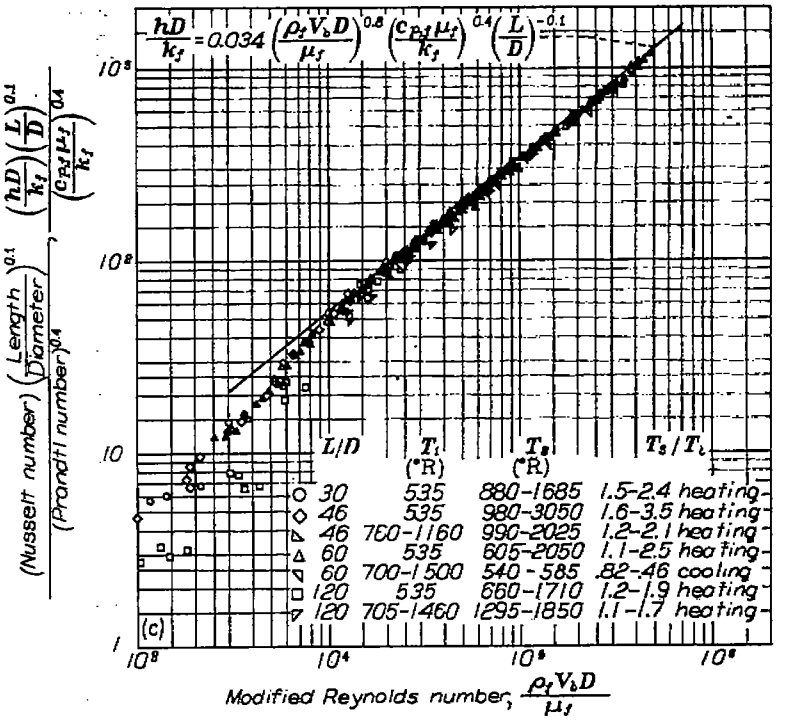

(c) Physical properties of air evaluated at film temperature T_f; thermal conductivity proportional to $\sqrt{T}$.

FIGURE 13.—Concluded. Summary plot of experimental data using modified method of correlating heat-transfer coefficients.

Figure 13 (c) shows the data of figures 13 (a) and 13 (b) replotted using the assumption that thermal conductivity varies as the square root of temperature, and with the physical properties and density evaluated at T_f. The line representing equation (15b) is included. The conductivity-temperature relation assumed in figure 13 (c) results in the best correlation of all the present data. Trends with respect to temperature level and with T_s/T_b for both heat addition and heat extraction are almost completely eliminated and the data can be represented by equation (15b).

CORRELATION OF FRICTION COEFFICIENTS

Friction coefficients without heat transfer.—Average half-friction coefficients $f/2$ calculated by equation (6) for flow without heat transfer are plotted against Reynolds number GD/μ_b in figure 14 (a). Included for comparison is the line representing the Kármán-Nikuradse relation between friction coefficient and Reynolds number for incompressible turbulent flow, which is

$$\frac{1}{\sqrt{8\frac{f}{2}}}=2\log\left(\frac{GD}{\mu_b}\sqrt{8\frac{f}{2}}\right)-0.8 \qquad (17)$$

and the line representing the equation for laminar flow in circular tubes, which is

$$\frac{f}{2}=\frac{8}{\frac{GD}{\mu_b}} \qquad (18)$$

Reasonably good agreement with the Kármán-Nikuradse line is obtained for all five configurations in the range of Reynolds number corresponding to turbulent flow. It is of interest that the Kármán-Nikuradse relation, which was derived for incompressible flow, applies with good accuracy to compressible flow, inasmuch as the present data cover a range of tube-exit Mach number up to 1.0.

Figure 14 (a) illustrates the agreement of the data obtained in the present investigation without heat transfer with the results of other investigators, which are in general agreement with equations (17) and (18).

Friction coefficients with heat addition.—Representative friction data, obtained with heat addition to the air, are shown in figure 14 (b). Data for no heat transfer (T_s/T_b, 1.0), and the Kármán-Nikuradse and laminar flow lines are included for comparison. These data are for an Inconel tube having a length-diameter ratio of 60 and a bellmouth entrance, and were obtained simultaneously with the heat-transfer data of figure 5.

The data for low surface temperatures (T_s, 605° and 675° R) agree fairly well with those for no heat addition. As the surface temperature is increased, however, $f/2$ decreases at high Reynolds numbers and stays the same or increases at low Reynolds numbers, so that the data cannot be represented by a single line. These results are typical of those obtained with other entrances and length-diameter ratios.

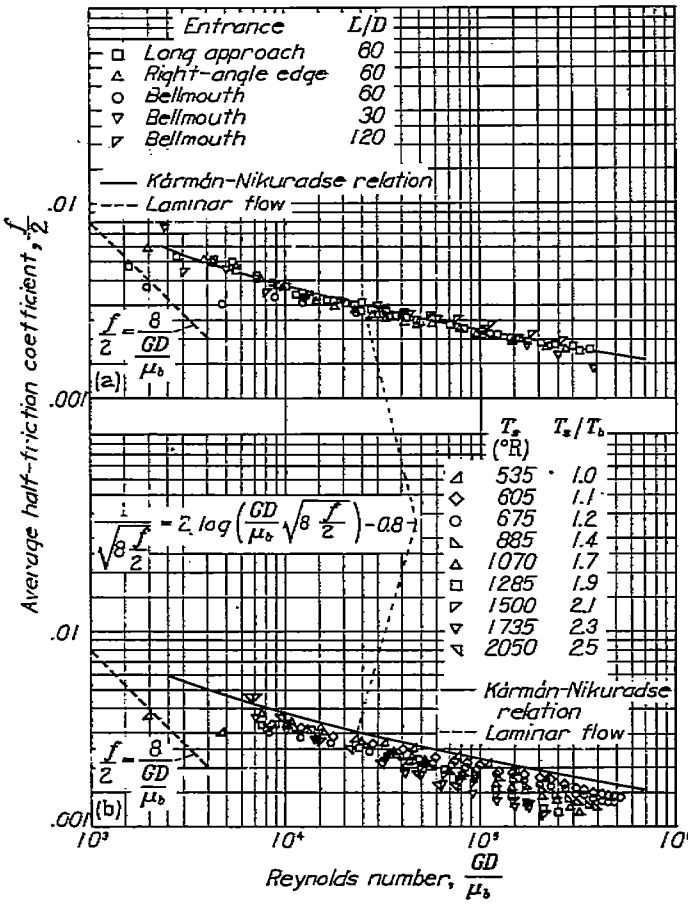

(a) No heat transfer; Inconel tubes; inlet-air temperature, 535° R.
(b) Heat addition; Inconel tube; length-diameter ratio, 60; bellmouth entrance; inlet-air temperature, 535° R.

FIGURE 14.—Variation of average half-friction coefficient with Reynolds number.

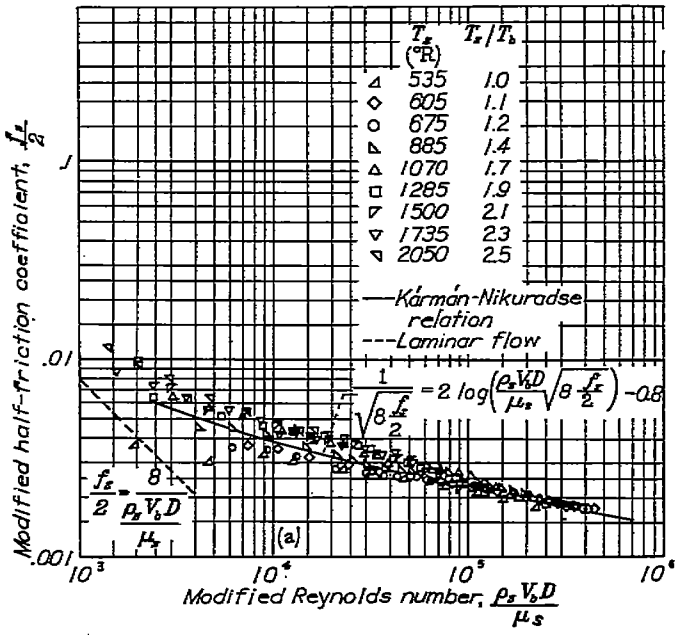

(a) Viscosity and density evaluated at surface temperature T_s.

FIGURE 15.—Variation of modified half-friction coefficient with modified Reynolds number with heat addition. Inconel tube; length-diameter ratio, 60; bellmouth entrance; inlet-air temperature, 535° R.

Modified friction coefficient.—Various methods of defining the Reynolds number and the dynamic pressure on which to base the average friction coefficient were tried in an attempt to eliminate the trends shown in figure 14 (b). One such method was to base the dynamic pressure on a density evaluated at the surface temperature and a velocity evaluated at the average air temperature and to plot the resulting friction coefficient against the modified Reynolds number $\rho_s V_b D/\mu_s$. The friction coefficient defined in the foregoing way f_s is given by equation (9).

The results of this method of correlating the friction data are illustrated in figure 15 (a), where $f_s/2$ is plotted against $\rho_s V_b D/\mu_s$. The data are the same as in figure 14 (b), and curves representing the Kármán-Nikuradse and the laminar flow equations are again included.

In general, the friction coefficient is overcorrected and increases with an increase in T_s/T_b at constant modified Reynolds number. Figure 15 (a) is typical of the results obtained with other entrances and length-diameter ratios.

The friction factor was also defined on the basis of a density evaluated at the film temperature T_f (equation (8)). The resulting friction coefficient was then plotted against the modified Reynolds number with the density and viscosity evaluated at the film temperature T_f. The data of figure 15 (a) are replotted in this manner in figure 15 (b). The trends with T_s/T_b are eliminated for Reynolds numbers above 20,000 and the data can be represented with reasonable accuracy by the Kármán-Nikuradse relation using modified parameters.

Effect of entrance configuration.—Friction data obtained simultaneously with the heat-transfer data of figure 8 using an Inconel tube (length-diameter ratio, 60) with long-approach and right-angle-edge entrances are shown in figure 16 (a). Data for no heat transfer are included. At Reynolds numbers above 20,000, the data of figure 16 (a) are in reasonable agreement with the Kármán line, which was seen in figure 15 (b) to fit the bellmouth-entrance data with good accuracy. The data for the right-angle-edge entrance fall slightly below the reference line. No particular significance can be attached to this small deviation, however, and it is felt that the average friction coefficients for all three entrances can be approximated with sufficient accuracy at modified Reynolds numbers greater than about 20,000 by the relation

$$\frac{1}{\sqrt{8\frac{f_f}{2}}}=2\log\left(\frac{\rho_f V_b D}{\mu_f}\sqrt{8\frac{f_f}{2}}\right)-0.8 \qquad (19)$$

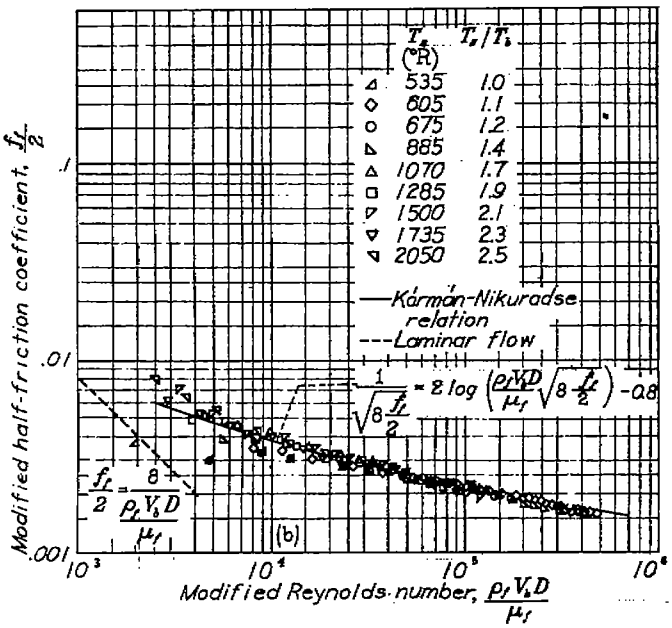

(b) Viscosity and density evaluated at film temperature T_f.

FIGURE 15.—Concluded. Variation of modified half-friction coefficient with modified Reynolds number with heat addition. Inconel tube; length-diameter ratio, 60; bellmouth entrance; inlet-air temperature, 535° R.

Effect of length-diameter ratio and inlet-air temperature.—Friction data obtained with heat addition to the air for length-diameter ratios of 30 and 120 and for inlet-air temperatures from 535° to 1460° R are shown in figure 16 (b). The data of figure 16 (b), which are for a bellmouth entrance, fall above the Kármán line, whereas the bellmouth data in figure 15 (b), which correspond to a length-diameter ratio of 60, fall on the line. No particular significance can be attached to these differences, however, and it is felt that the data for the range of length-diameter ratio and inlet-air temperature considered can be represented with sufficient accuracy by equation (19).

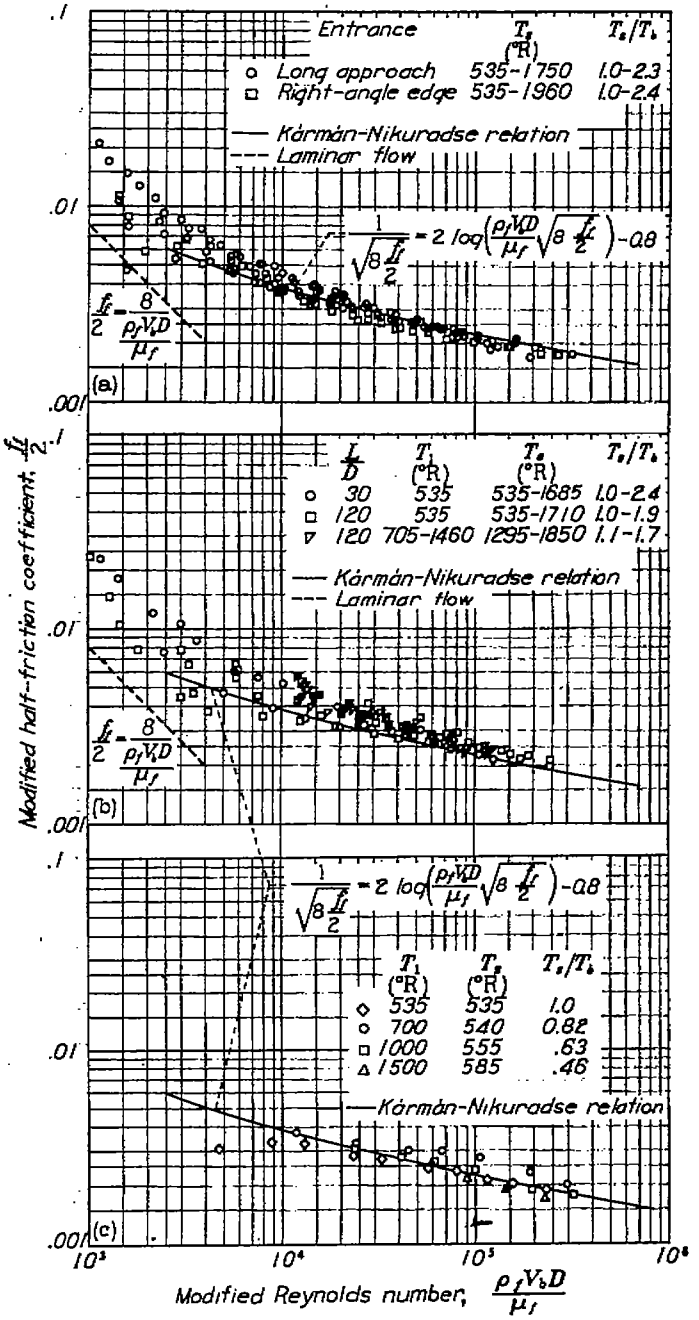

(a) Effect of entrance configuration with heat addition. Inconel tube; length-diameter ratio, 60; inlet-air temperature, 535° R.

(b) Effect of length-diameter ratio and inlet-air temperature with heat addition. Inconel tubes.

(c) Effect of heat extraction. Inconel tube; length-diameter ratio, 60.

FIGURE 16.—Variation of modified half-friction coefficient with modified Reynolds number.

Effect of heat extraction.—Friction coefficients obtained simultaneously with the data of figure 11 for heat extraction from the air are shown in figure 16 (c). Data for no heat transfer are included. The coordinates and the reference line are the same as in figures 15 (b) to 16 (b). The data can be represented with reasonable accuracy by the reference line for turbulent flow.

SUMMARY OF RESULTS

The results of this investigation of heat transfer and associated pressure drops conducted with air flowing through smooth tubes for a range of surface-to-air temperature ratio from 0.46 to 3.5, surface temperature from 535° to 3050° R, inlet-air temperature from 535° to 1500° R, Reynolds number up to 500,000, exit Mach number up to 1.0, length-diameter ratio from 30 to 120, and for three entrance configurations may be summarized as follows:

1. Conventional methods of correlating average heat-transfer coefficients, wherein specific heat, viscosity, and thermal conductivity are evaluated at the average air temperature, resulted in a considerable and progressive separation of the data with increased surface-to-air temperature ratio for heat addition to the air. Evaluation of the physical properties at the film or surface temperature, instead of the bulk temperature, aggravated the separation.

2. Satisfactory correlation of heating data obtained with inlet-air temperatures near 535° R was obtained for the range of surface temperature considered when the Reynolds number was modified by substituting the product of air density evaluated at the surface temperature and velocity evaluated at the average total air temperature for the conventional mass flow per unit cross-sectional area, and the properties of the air were evaluated at the average surface temperature.

3. Correlation of the heating data obtained at inlet-air temperatures above 535° R by the modified method resulted in a decrease in Nusselt number for an increase in average air temperature, which was eliminated by the assumption that the thermal conductivity of air varies as the square root of temperature and by the evaluation of the physical properties of air including density at a temperature midway between air and surface temperatures instead of at the surface temperature.

4. With the assumption that thermal conductivity varies as the square root of temperature, data obtained for cooling of the air indicated that the effect of surface-to-air temperature ratio was the same as for heat addition, so that both heating and cooling data can be represented by the same equation.

5. The use of different entrances to the test section (that is, a long-approach, a right-angle-edge, or a bellmouth entrance) had negligible effect on average heat-transfer coefficients, at least for length-diameter ratios of 60 or greater.

6. Variation in tube length-diameter ratio had a relatively small effect on average heat-transfer coefficients, which was satisfactorily accounted for by including a parameter for length-diameter ratio in the correlation equation.

7. Friction coefficients for no heat transfer, calculated from a dynamic pressure based on an average air density, were in good agreement with those obtained by other investigators. The corresponding friction coefficients obtained with heat addition to the air showed a considerable effect of surface-to-air temperature ratio for the Reynolds numbers in the turbulent region.

8. All the friction data could be represented with reasonable accuracy by the Kármán-Nikuradse relation for incompressible turbulent flow by using a friction coefficient calculated from a dynamic pressure based on a density evaluated at the film temperature and the modified Reynolds number in which the density and viscosity were evaluated at a temperature midway between the air and surface temperatures.

LEWIS FLIGHT PROPULSION LABORATORY
NATIONAL ADVISORY COMMITTEE FOR AERONAUTICS
CLEVELAND, OHIO, *December 31, 1950*

REFERENCES

1. Nusselt, Wilhelm: Der Einfluss der Gastemperatur auf den Wärmeübergang im Rohr. Techn. Mechan. u. Thermodynamik, Bd. 1, Nr. 8, Aug. 1930, S. 277–290.
2. McAdams, William H.: Heat Transmission. McGraw-Hill Book Co., Inc., 2d ed., 1942.
3. Humble, Leroy V., Lowdermilk, Warren H., and Grele, Milton: Heat Transfer from High-Temperature Surfaces to Fluids. I—Preliminary Investigation with Air in Inconel Tube with Rounded Entrance, Inside Diameter of 0.4 Inch, and Length of 24 Inches. NACA RM E7L31, 1948.
4. Lowdermilk, Warren H., and Grele, Milton D.: Heat Transfer from High-Temperature Surfaces to Fluids. II—Correlation of Heat-Transfer and Friction Data for Air Flowing in Inconel Tube with Rounded Entrance. NACA RM E8L03, 1949.
5. Lowdermilk, Warren H., and Grele, Milton D.: Influence of Tube-Entrance Configuration on Average Heat-Transfer Coefficients and Friction Factors for Air Flowing in an Inconel Tube. NACA RM E50E23, 1950.
6. Desmon, Leland G., and Sams, Eldon W.: Correlation of Forced-Convection Heat-Transfer Data for Air Flowing in Smooth Platinum Tube with Long-Approach Entrance at High Surface and Inlet-Air Temperatures. NACA RM E50H23, 1950.
7. Tribus, Myron, and Boelter, L. M. K.: An Investigation of Aircraft Heaters. II—Properties of Gases. NACA ARR, Oct. 1942.
8. Boelter, L. M. K., and Sharp, W. H.: An Investigation of Aircraft Heaters. XXXII—Measurement of Thermal Conductivity of Air and of Exhaust Gases Between 50° and 900° F. NACA TN 1912, 1949.
9. Keenan, Joseph H., and Kaye, Joseph: Thermodynamic Properties of Air. John Wiley & Sons, Inc., 1945.
10. Gröeber, H., und Erk, S.: Die Grundgesetze der Wäermeübertrangung. Julius Springer (Berlin), 1933.
11. Bernardo, Everett, and Eian, Carroll S.: Heat-Transfer Tests of Aqueous Ethylene Glycol Solutions in an Electrically Heated Tube. NACA ARR E5F07, 1945.
12. Deissler, Robert G.: Analytical Investigation of Turbulent Flow in Smooth Tubes with Heat Transfer with Variable Fluid Properties for Prandtl Number of 1. NACA TN 2242, 1950.
13. Cholette, Albert: Heat Transfer—Local and Average Coefficients for Air Flowing Inside Tubes. Chem. Eng. Prog., vol. 44, no. 1, Jan. 1948, pp. 81–88.